ELSEVIER

Biophysical Chemistry 99 (2002) 155–168

Biophysical Chemistry

www.elsevier.com/locate/bpc

Dynamic hydration numbers for biologically important ions

Michael Y. Kiriukhin, Kim D. Collins*

Department of Biochemistry and Molecular Biology, University of Maryland Medical School, 108 N. Greene Street, Baltimore, MD 21201-1503, USA

Received 24 May 2002; accepted 29 May 2002

Abstract

The role of ionized groups in biological systems is determined by their affinity for water [Biophys. J. 72 (1997) 65–76]. The tightly bound water associated with biologically important ions increases their apparent size. We define the apparent dynamic hydration number of an ion here as the number of tightly bound water molecules that must be assigned to the ion to explain its apparent molecular weight on a Sephadex® G-10 size exclusion column, and report the first accurate determination of tightly bound water for 23 ions of biological significance, including H^+ and HO^-. We also calculate the radius of the equivalent hydrated sphere (r_h) for each ion. We find that the ratio of the hydrated volumes of two ions approximates the ratio of the square of the charges of the same two ions. Since the 'ionic strength' of the solution also depends upon the square of the charges on the ions, our results suggest that ionic strength effects may largely arise from local effects related to the hydrated volume of the ion—that is, from space filling, osmotic, water activity, surface tension and hydration shell overlap effects rather than from long-range electric field effects.

Keywords: Hydroxide hydration; Ion hydration; Ionic strength; Magnesium hydration; Phosphate hydration; Hydrated proton

1. Introduction

Specific ions at moderate to high concentrations in aqueous solution can have large but very different effects on the behavior of other solutes. For example, malonate is much more effective than other common anions in crystallizing a wide range of proteins [1]. Thiocyanate is particularly effective in crystallizing the basic protein lysozyme, but phosphate is not, while phosphate is especially effective in crystallizing the acidic protein collagenase, but chloride is not [2]. Complex ion-specific effects in fractionating proteins by ion exchange are common [3], while the ion-specific retention of ribonuclease on a hydrophobic interaction chromatography column follows the Hofmeister series [4]. The physical basis for these dramatically different behaviors is poorly understood. We have chosen to investigate the origins of these and other ionic phenomena by examining the affinity of 23 biologically significant ions for water. The hydrated size of biological ions, reported here as a dynamic hydration number and a radius of the

*Corresponding author. Tel.: +1-410-706-7199; fax: +1-410-706-8297.

E-mail address: kcollins@umaryland.edu (K.D. Collins).

0301-4622/02/$ - see front matter © 2002 Elsevier Science B.V. All rights reserved.
PII: S0301-4622(02)00153-9

equivalent hydrated sphere, specifies the distance over which the electric field of the ion controls solvent behavior, identifies the water molecules accepting charge from the ion, defines solvent shell structure, determines the distance over which the osmotic attractive force between protein molecules or other particles acts, affects the activity coefficient of test solutes in the solution (see below), and modulates the magnitude of space filling, surface tension and viscosity effects. Dynamic hydration numbers (or related measures of hydrated ion size), sometimes called transport numbers or other names, have been reported before [5–12], but have varied widely and usually been unrealistically high. They have almost always (incorrectly) assigned positive values to chaotropes [chaotropes are defined in point (iv), Section 3.6]. The values reported here in Tables 1 and 2 are consistent with viscosity *B* coefficients, neutron and X-ray diffraction studies, and other physical measures of ion hydration [13,14]. In general, the dynamic hydration numbers correlate well with charge density, with higher charge density being associated with higher dynamic hydration number.

2. Materials and methods

All chemicals were analytical or reagent grade. Polymers of glycine and glutamate were purchased from Sigma. Sephadex G-10 (Amersham Pharmacia Biotech, lot number KA33825) was prepared according to Washabaugh and Collins [15]. A Shimadzu UV-2401PC UV-Vis recording spectrophotometer was used for all spectral determinations. A jacketed cylindrical glass column (XK-16, Amersham Pharmacia Biotech) at 30 °C was packed using a peristaltic pump for 5 days at 135 ml cm^{-2} h^{-1}, and then continually fed by gravity at 1.2 ml min^{-1}. The final column bed was 1.6 cm in diameter by 98 cm high and the fractionating volume was 120 fractions (78 ml). For quantitative work, the column was fed by gravity at 1.2 ml min^{-1} and 30 °C; 0.65-ml fractions were collected. Each compound analyzed was run as a 0.6-ml sample at 0.1 M. Results are reported as the partition coefficient (relative elution position), K_D, defined as $K_D=(V_e-V_o)/(V_i-V_o)$, where V_o is the excluded (void) volume, V_i is the included volume and V_e is the elution volume for a given solute. The H_2O 'included volume' of the column ($K_D=1$) was determined measuring the ^3HOH included volume and multiplying by 0.917 to convert it to the $H_2^{18}O$ included volume [16]. For calculations, H_2O was assigned a molecular weight of 18. The 'excluded volume' of the column ($K_D=0$) was measured as the peak elution position of polyglutamic acid (MW = 13 700) spectrophotometrically determined at 205 nm. Homopolymers of glycine, ranging from glycylglycine ($n=2$) to hexaglycine ($n=6$), were used as calibration standards and were also spectrophotometrically detected at 205 nm. Each chemical species was determined by a specific assay for that substance. [^{32}P]-orthophosphoric acid, ^{22}NaCl, Na^{35}Cl, $^{45}CaCl_2$ and [^{14}C]-formic acid (Amersham Pharmacia Biotech) were detected by liquid scintillation counting. Zn^{2+}, SO_4^{2-} and Al^{3+} were detected with water analysis kits (Hach Company, Loveland, CO). Ba^{2+}, Sr^{2+}, Be^{2+} and F^- were colorimetrically detected according to Marczenko [17]. Li^+ was detected using vitros Li slides (Johnson & Johnson Clinical Diagnostics Inc, Rochester, NY). Mg^{2+} was detected by Mag-Fura 2 fluorescent indicator (Molecular Probes, Eugene, OR). Cr^{3+} was spectrophotometrically detected at 418 nm (fresh solution) or 410 nm (aged solution). H^+ and OH^- were detected by titration using bromothymol blue as indicator. Each sample and standard was run in triplicate, with no variation in the identity of the peak fraction.

3. Results and discussion

3.1. Using size exclusion chromatography to determine hydrated ion size

We have previously shown that aqueous size exclusion chromatography in its simplest form (inexpensive chromatographic media in a gravity-fed column of modest size at room temperature and atmospheric pressure) can be used to obtain dynamic hydration numbers for single ions [18], and we extend that work here. Sephadex G-10 is epichlorohydrin-cross-linked dextran in beaded form, which is meant to separate solutes up to a molecular weight of approximately 700 by size

exclusion: large molecules are excluded by the small pore size of the beads, taking a short path through the column and emerging early, while small molecules penetrate the beads, taking a long path through the column and emerging late. The apparent dynamic hydration number (ADHN) of an ion is the number of tightly bound water molecules that move with an ion as it diffuses, and as determined here is simply the number of tightly bound water molecules that must be assigned to an ion to explain its apparent molecular weight on a Sephadex G-10 size exclusion column. The joint motion of water and ion requires that the bound water diffuse more slowly than pure water, and that the water-ion complex have a lifetime of at least several ps at room temperature [19–22,85]. The mean lifetime of attachment of a water molecule to K^+ [apparent dynamic hydration number (ADHN) = 0] has been calculated to be 2 ps, 5 ps for Na^+ (ADHN = 0.22), 27 ps for Li^+ (ADHN = 0.6) and approximately 10^6 ps for Mg^{2+} (ADHN = 5.73) [85]. The rates of water exchange for many other metal ions have also been estimated [22]. For all the ions examined, except Cr^{3+} and perhaps Al^{3+}, we expect water exchange on the ion to be fast compared to transport processes associated with flow through the gel sieving column (a flow rate of 1.2 ml min^{-1} was used), and we have previously shown that the elution position of the strongly hydrated salts NaF and Na_2SO_4 does not change over the temperature range of 2.5–50 °C (the elution position of NaCl is not temperature-dependent either) [15]. $AlCl_3 \cdot 6H_2O$ and $CrCl_3 \cdot 6H_2O$ were the beginning salts used to characterize Al^{3+} and Cr^{3+}. Freshly dissolved $CrCl_3 \cdot 6H_2O$ in particular shows a slow water exchange reaction requiring many hours to complete [23,24]; it is associated with a change in color. Thus, we determined the elution position of $CrCl_3 \cdot 6H_2O$ immediately after dissolution ($\lambda_{max} = 418$ nm) and after 1 week in solution ($\lambda_{max} = 410$ nm); the elution position was unchanged.

Two assumptions are required to obtain the dynamic hydration number and radius of the equivalent hydrated sphere (r_h) from size exclusion chromatography. First, although the column measures a volume (or, more rigorously, a partition coefficient), we calibrate the column with standards described by their molecular weight (MW), and plot the partition coefficient (relative elution position) K_D vs. the log of the molecular weight, because for spherical molecules or random coils, it has been empirically found that the molecular weight can be expressed in terms of some power of the Stokes radius [25]. This interconversion between weight and volume assumes a constant density, and the density of water at 30 °C is used for this because water is used to generate the calibration curve in Fig. 1a, and thus to define ideal behavior. Second, the column generates an apparent molecular weight for a neutral salt, and the excess molecular weight (in the form of tightly bound water molecules) is apportioned between the ions of the salt using a mixed salt containing either the weakly hydrated cation K^+ or the weakly hydrated anion Cl^-, which are marginally chaotropes and do not adsorb detectably to the column [14,15,18], plus a strongly hydrated ion to which the tightly bound water molecules are assigned.

Fig. 1a uses H_2O and glycine polymers from diglycine ($n = 2$) to hexaglycine ($n = 6$) to define ideal behavior—i.e. solutes that bind water with affinity equal to the affinity of water for itself in bulk solution. The enthalpy of interaction of the amide group with water is approximately −11.5 kcal mol^{-1} [26], while the heat of evaporation of water at 20 °C is 10.5 kcal mol^{-1} [27]; thus, the strength of amide–water interactions is approximately equal to the strength of water–water interactions. The key to an accurate calibration of the Sephadex G-10 column is to use standards that cover the whole molecular-weight fractionating range of the column, which we have done. Inspection of Fig. 1a shows that the elution positions of the standards are all on a straight line. However, slight non-ideality in the glycine oligomers can be detected: there is a very small bias towards the standards being too large as they grow smaller. Since the carboxylate binds two water molecules tightly (Table 1), the glycine oligomers carry two water molecules with them at the carboxyl terminus; these two water molecules increase the effective molecular weight slightly, and this effect is relatively larger for the shorter glycine oligomers.

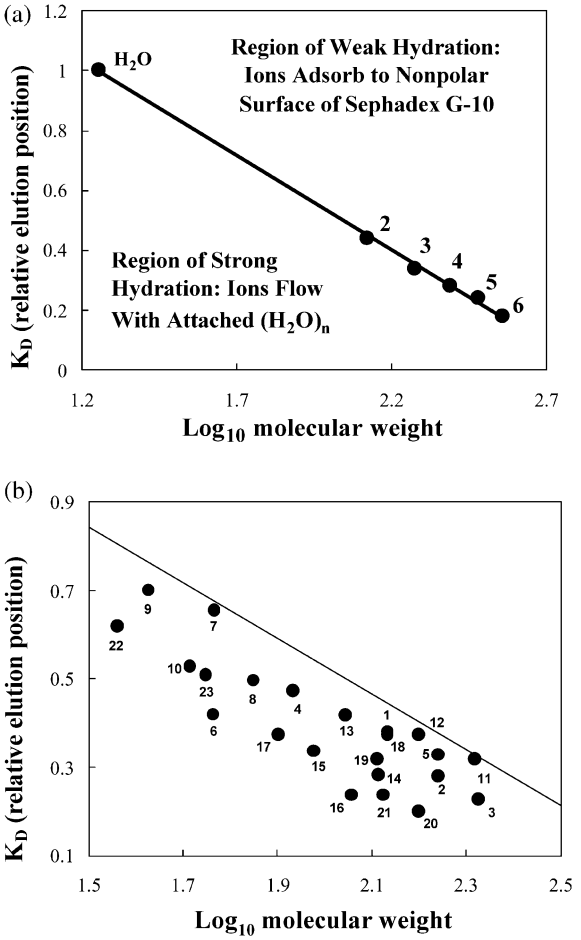

Fig. 1. (a) Calibration of the Sephadex G-10 column with H_2O and glycine homopolymers. H_2O refers to $H_2^{18}O$ and the numbers 2–6 refer to the peptides glycylglycine–hexaglycine (see Section 2 for the definition of K_D and other information). (b) The apparent molecular weight of neutral salts as determined on the Sephadex G-10 column. The apparent excess molecular weight associated with each salt is measured by its horizontal displacement from the calibration curve. The numbered data points correspond to the entries in Tables 1 and 2.

We have found that neutral carbohydrate oligomers bind weakly to Sephadex G-10 and that the glycine oligomers give the best column calibration. Weakly hydrated ions adsorb to the non-polar surface of the gel and have apparent molecular weights smaller than their anhydrous molecular weight (above the calibration line in Fig. 1a), while strongly hydrated ions diffuse with attached water molecules through the column by gel sieving and have apparent molecular weights larger than their anhydrous molecular weights (below the calibration line in Fig. 1a). We know that the calibration line shown in Fig. 1a is accurately positioned for two reasons. First, ions with negative viscosity *B* coefficients chromatograph above the line, while ions with positive viscosity *B* coefficients chromatograph below the line [14,18]. And second, the behavior of ions changes at the calibration line: those salts found above the line show concentration- and temperature-*dependent* elution (characteristic of adsorption), while those found below the line show concentration- and temperature-*independent* elution (characteristic of gel sieving) [15]. Fig. 1b shows the excess molecular weight (horizontal displacement from the calibration line) associated with each salt, and the numbered points in Fig. 1b correspond to the numbered entries in Tables 1 and 2, which are presented as ion-specific apparent dynamic hydration numbers (ADHN) and ion-specific radii of the equivalent hydrated spheres (r_h). The effective molecular weight of NaCl (anhydrous molecular weight, 58.45) on the Sephadex G-10 column is 62.4 for a 0.1 M sample of ^{22}NaCl or Na^{35}Cl eluted with either 0.1 M NaCl or water, and this excess molecular weight is attributed to 0.22 water molecules bound to the Na^+ ion (Table 1). Neither does the effective molecular weight of NaCl change when a dilute 1 mM sample of ^{22}NaCl is eluted with either 0.1 M NaCl or water (data not shown). Furthermore, the apparent molecular weight of hydrated Na^+ (anhydrous molecular weight, 23.0) is 26.9 within experimental error when determined as either sodium chloride or sodium formate. Similarly, the dynamic hydration numbers of Li^+, Ca^{2+} or Mg^{2+} do not differ between the chloride or formate salt. From these control experiments, we draw the following three conclusions. First, because the apparent molecular weight of NaCl is slightly greater than the anhydrous molecular weight and does not depend on which ion is labeled with radioactivity, we conclude that only neutral salts penetrate the sieving gel (not separate ions alone). Second, because the apparent molecular weight of NaCl

Table 1
Apparent dynamic hydration number and radius of equivalent hydrated sphere for biological ions at 30 °C (uncorrected for electrostriction)

Species determined (0.1 M)		Crystal radius (Å) (CN)[h]	r_h (Å)[i]	ADHN[k,j]	Counterion	Eluant salt (0.1 M)
1	$H_2PO_4^-$	2.38[a]	3.02	1.91±0.17	K^+	KCl
2	HPO_4^{2-}	2.30[a]	3.27	3.95±0.23	K^+	KCl
3	PO_4^{3-}	2.23[a]	3.39	5.10±0.28	K^+	KCl
4	HCO_2^-	1.31[a]	2.58	2.00±0.12	K^+	KCl
5	SO_4^{2-}	2.15[a]	3.00	1.83±0.20	K^+	KCl
	Cl^-[b]	1.81 (6)[g]	(1.95)	0 (assigned)		
6	F^-	1.19 (6)[c]	2.84	5.02±0.14	K^+	KCl
	NH_4^+[d]	1.61 (6)[g]	(1.04)	0 (assigned)		
	K^+[e]	1.38 (6)[g]	(2.01)	0 (assigned)		
7	Na^+	1.02 (6)[g]	1.78	0.22±0.06	Cl^-	NaCl
	Na^+	1.02 (6)[g]	1.78	0.22±0.06	Cl^-	H_2O
8	Na^+	1.02 (6)[g]	1.83	0.30±0.13	HCO_2^-	$Na^+HCO_2^-$
	Na^+ (as $[^{35}Cl^-]$)	1.02 (6)[g]	1.78	0.22±0.06	Cl^-	NaCl
	Na^+ (as $[^{35}Cl^-]$)	1.02 (6)[g]	1.78	0.22±0.06	Cl^-	H_2O
9	Li^+	0.76 (6)[g]	1.55	0.58±0.05	Cl^-	KCl
10	Li^+	0.76 (6)[g]	1.58	0.64±0.06	HCO_2^-	$K^+HCO_2^-$
11	Ba^{2+}	1.52 (10)[g]	3.11	0.35±0.25	Cl^-	KCl
12	Sr^{2+}	1.36 (10)[g]	2.80	0.95±0.16	Cl^-	KCl
13	Ca^{2+}	1.23 (10)[m]	2.53	2.09±0.14	Cl^-	KCl
14	Ca^{2+}	1.23 (10)[m]	2.60	2.38±0.16	HCO_2^-	$K^+HCO_2^-$
15	Mg^{2+}	0.72 (6)[g]	3.00	5.85±0.19	Cl^-	KCl
16	Mg^{2+}	0.72 (6)[g]	3.00	5.73±0.18	HCO_2^-	$K^+HCO_2^-$
17	Be^{2+}	0.27 (4)[g]	2.80	5.31±0.16	Cl^-	KCl
18	Zn^{2+}	0.74 (6)[g]	2.80	2.18±0.16	Cl^-	KCl
19	Ni^{2+}	0.60 (6)[g]	3.11	4.71±0.20	Cl^-	H_2O
20	Cr^{3+}[f]	0.62 (6)[g]	3.61	9.59±0.31	Cl^-	KCl
21	Al^{3+}	0.54 (6)[g]	3.37	8.68±0.27	Cl^-	KCl

[a] Derived from Pauling [28].
[b] Cl^- is a chaotrope [14,18,29].
[c] Cotton et al. [24].
[d] NH_4^+ is a chaotrope [14,18,30].
[e] K^+ is a chaotrope [13,14,18,31].
[f] Result identical for fresh and aged solution.
[g] Crystal radii from Richens [23].
[h] The coordination number (CN) is the number of water molecules in the first hydration shell.
[i] Radius of equivalent hydrated sphere, r_h, is calculated from the molecular mass of the ion using the density of H_2O at 30 °C to convert from mass to volume.
[j] Error brackets calculated from the size of the fraction collected.
[k] ADHN, apparent dynamic hydration number.
[m] Neilson and Enderby [21].

does not change even at low concentration and in the absence of supporting electrolyte, we conclude that there are no ion exchange effects of the salts with the gel. And third, because the apparent dynamic hydration numbers for Na^+, Li^+, Ca^{2+} and Mg^{2+} do not differ when determined as either the chloride or formate salt, we conclude that the apparent dynamic hydration number of strongly hydrated ions is not counterion-dependent at these concentrations.

Table 2
Apparent dynamic hydration number and radius of equivalent hydrated sphere for H^+ and OH^- at 30 °C (uncorrected for electrostriction)

Species determined (0.1 M)		Crystal radius (Å) (CN)[f]	r_h (Å)[b]	ADHN[a]	Counter ion	Eluant salt (0.1 M)
22	H^+		1.96	1.93 ± 0.07	Cl^-	KCl
	H^+		1.96	1.93 ± 0.07	Cl^-	H_2O
23	OH^-	1.35 (4)[e]	2.41	2.80 ± 0.10	K^+	KCl
	OH^-	1.35 (4)[e]	2.41	2.80 ± 0.10	K^+	H_2O
24	H_2O	1.38[d]	(1.55)[c]			

[a] ADHN, apparent dynamic hydration number
[b] Radius of equivalent hydrated sphere.
[c] Calculated from density of H_2O at 30 °C (0.99567 g/ml) [32].
[d] Lonsdale [33].
[e] Richens [23].
[f] The coordination number (CN) is the number of water molecules in the first hydration shell.

3.2. The issue of electrostriction

Water molecules near polar solutes take up less space than those near apolar atoms or in bulk solution [34], and this electrostriction has been the object of much study ([35], [36] and references therein; [37]). Because solution X-ray diffraction of Mg^{2+} in water shows six water molecules in the first hydration layer, but no large alteration in the density of the second hydration layer [38], Mg^{2+} has a maximum of six tightly bound water molecules in solution. Since any substantial correction of our apparent dynamic hydration number of 5.8 for Mg^{2+} in Table 1 for electrostriction would indicate the presence of more than six tightly bound water molecules, we conclude that no such correction is necessary, and thus our results in Table 1 are presented with no correction for electrostriction. Comparison of our apparent dynamic hydration number for Cr^{3+} with solution neutron [39] and X-ray [40] diffraction data, and of our apparent dynamic hydration number for Be^{2+} with ab initio molecular orbital calculations [41] also suggest that a correction for electrostriction is unnecessary (see below). We recognize the existence and importance of electrostriction, but this phenomenon seems to be already contained in our Sephadex G-10-derived apparent dynamic hydration numbers.

3.3. Strongly bound water as determined by Sephadex G-10 chromatography correlates well with solvent density perturbation measured by solution X-ray and neutron diffraction, as well as with results from other physical techniques and simulations

Difference solution X-ray and neutron diffraction studies of simple ions in water can be performed when two stable isotopes of the ion are available. These studies generate radial distribution functions, which show solvent density perturbations as a function of distance from the center of the scattering ion. Both oxygen and deuterium scatter neutrons; thus, neutron diffraction of ions in D_2O can detect solvent that is strongly oriented, as well as strongly bound [13]. A large solvent density perturbation is associated with strongly bound and oriented D_2O; as the solvent density perturbation disappears, so does the preferential orientation of the now weakly bound D_2O [13]. Our apparent dynamic hydration numbers for Li^+, Na^+, K^+, Zn^+, Ni^{2+}, Mg^{2+} and Cr^{3+}, which reflect the charge density of each ion, correlate well with their solution neutron-diffraction solvent density perturbations [13,38], suggesting that both techniques are measuring tightly bound water. The most informative points of comparison between techniques are where natural discontinuities occur:

the change from weak to strong hydration between K^+ and Na^+; the change from weak to strong second-shell hydration between Mg^{2+} and Be^{2+} or Cr^{3+}; and the change from an inner sphere coordination number of six for Mg^{2+} to four for Be^{2+}.

The water distribution around the mono-anionic phosphate in DNA has been studied by crystallographic X-ray diffraction; an examination of 59 crystal structures found six hydration sites in a cone shape around the two oxygens over which the single negative charge is distributed [42]. We see two of these six water molecules as tightly bound in our gel sieving experiments. An analysis of X-ray crystal structures of small molecules found that carboxylate groups, on average, accept six hydrogen bonds [43], with the hydrogen atoms clustering in the carboxylate lone-pair directions [44]. Computational studies found that the six water molecules hydrogen bonding to the carboxylate accounted for 40% of the enthalpy change associated with bulk solvation [45], with only a slight preference for the *syn* lone pairs (those lone pairs nearest the neighboring oxygen) [46]. The charge density on the two oxygens of the carboxylate are probably comparable to the charge density on the two oxygens of the phosphate mono-anion, and we also see two of the six carboxylate-associated water molecules as being tightly bound in our gel sieving experiments. However, examination of small molecule crystals indicates that 'In general, preferential phosphate–Lewis acid geometry contrasts markedly with carboxylate–Lewis acid geometry' [47]. Di-anionic sulfate binds only two water molecules tightly, while di-anionic phosphate binds four water molecules tightly. However, the two negative charges of the phosphate are spread over three oxygens, while the two negative charges of the sulfate are spread over four oxygens. Furthermore, sulfur is more electronegative than phosphate. Therefore, more negative charge is being pulled out of the central phosphorus atom than out of the central sulfur atom [28], and the charge density of the di-anionic phosphate oxyanions is higher than that of the di-anionic sulfate oxyanions. Hydrogen bonding patterns of both phosphate [47] and sulfate [48] have also been examined in small molecule crystals. Fluoride functions as an analog of hydroxide in biological systems, but the slightly smaller size of F^- (Table 1) generates a significantly higher apparent dynamic hydration number (5 for F^- and 3.6 for OH^-).

The apparent dynamic hydration numbers increase with increasing charge density within the IA cations (Na^+, Li^+, H^+) and within the IIA cations (Ba^{2+}, Sr^{2+}, Ca^{2+}, Mg^{2+}, Be^{2+}) up to Mg^{2+}. For example, Table 1 shows that 2.1 of the 10 water molecules in the first hydration shell of Ca^{2+} [49] are tightly bound. However, the apparent dynamic number decreases in going from Mg^{2+} (ADHN = 5.8) to Be^{2+} (ADHN = 5.3). Since the coordination number of the first hydration shell changes from $6H_2O$ for Mg^{2+} [50] to $4H_2O$ for Be^{2+} ([41] and references therein), we conclude that Be^{2+} contains 1.3 tightly bound water molecules in the second hydration shell (ADHN of 5.3 minus the 4 water molecules in the first hydration shell), consistent with the ab initio molecular orbital calculations of Bock and Glusker [41]. Thus, Be^{2+} appears to be the ion of lowest charge density for which strongly bound second-shell water has now been demonstrated. Our apparent dynamic hydration number for Be^{2+}, which by extrapolation from Mg^{2+} would have been expected to be above six for a hexa-coordinated Be^{2+}, accurately reflects the reduction in inner sphere coordination number for Be^{2+}, and illustrates that counting bound water molecules by Sephadex G-10 chromatography correlates closely with ab initio molecular orbital calculations. Cr^{3+} contains $6H_2O$ in the first [39,40] and $13H_2O$ in the second hydration shell [40,51]. Evidence for tightly bound water in the second hydration shell comes from neutron [39] and X-ray diffraction studies of aqueous solutions [40], ^{17}O-NMR and molecular dynamics calculations [52], molecular dynamics calculations alone [53], and IR spectroscopy [54]. We find 3.6 of the 13 Cr^{3+} second-shell water molecules to be tightly bound. Al^{3+} also has $6H_2O$ in the first hydration shell [23] and strong second shell hydration, as judged by far-infrared spectroscopy [55]. We find 2.7 tightly bound water molecules in the second hydration shell of Al^{3+}.

3.4. How strongly hydrated are H^+ and OH^-?

The apparent dynamic hydration number of 1.9 for the proton in Table 2 indicates that the major species in solution is the protonated water dimer $H_5O_2^+$ proposed by Zundel [56] rather than the protonated water tetramer $H_9O_4^+$ favored by Eigen [57], and is consistent with several recent computational analyses [58–60]. The apparent dynamic hydration number for hydroxide in Table 2 is 2.8, suggesting that the trihydrate is the most important form; modeling studies find stable tri- and tetrahydrate forms [61–63]. Table 2 also shows that neither the proton nor the hydroxide dynamic hydration number changes in going from water to 0.1 M KCl. Plausible estimates exist for the electrostriction associated with dissolved H^+ [64] and OH^- [65], but comparisons of our apparent dynamic hydration numbers for Mg^{2+}, Be^{2+} and Cr^{3+} with solution neutron diffraction data [13,38] and ab initio molecular orbital calculations [41] suggest that corrections for electrostriction to our Sephadex G-10-derived numbers are not necessary (see above).

3.5. 'Ionic strength' is an experimental observation

Ions in moderate to high concentration in water are known to interfere with the solvation of test solutes, resulting, for example, in the decreased dissociation and solubility of marginally soluble salts. Ionic strength was an experimental observation of G.N. Lewis and M. Randall in 1921 [66], who noted that ''In dilute solutions the activity coefficient of a given strong electrolyte is the same in all solutions of the same ionic strength.'' Ionic strength was defined by:

$$I = [\sum_i M_i \cdot z_i^2]/2$$

where M_i is the molarity of each ion, z_i is the charge on each ion and I is the ionic strength. (Ionic strength was originally defined in terms of molality.) The concept of ionic strength was subsequently rationalized by Debye and Hückel [67,68] using the model of continuum electrostatics.

3.6. The assumptions of continuum electrostatics are inconsistent with known data

The assumptions of continuum electrostatics, as listed below, are not consistent with many different kinds of experimental data. Continuum electrostatics assumes that:

i. Ions can be represented by point charges—i.e. the charge density of ions can be ignored and ion-specific effects for ions of the same sign and charge do not exist. This assumption occurs because continuum electrostatics does not use the strength of water–water interactions as a reference energy level. However, it is the ratio of the strength of ion-water interactions to the strength of water–water interactions that controls the behavior of ions in biological systems [14]. Dramatic ion-specific effects are common; for example, it is estimated that 25–40% of brain energy utilization may be related to Na^+,K^+-ATPase activity, which pumps K^+ into cells and Na^+ out. It is also the difference in charge density that makes intracellular calcium toxic but intracellular magnesium essential [14]. Assigning a finite size to ions in continuum electrostatics calculations does *not* address this issue.

ii. Ionic solutions can be conceptually separated into point charges and a continuum characterized by a fixed dielectric constant. However, there is substantial charge transfer to solvent from ions of high charge density to their tightly bound water molecules; for Mg^{2+}, fully $+0.82$ (i.e. more than 40% of the total charge) is transferred to the six tightly bound water molecules [50]; thus the water bound to Mg^{2+} has dramatically altered properties as compared to the water in bulk solution, and appears to play an important role in the function of Mg^{2+}. Mg^{2+} is usually required for the stabilization of compact RNA structures and typically remains mostly hydrated; in fact, fully hydrated $Mg^{2+}\cdot 6H_2O$ is a cofactor for several ribozymes and protein enzymes [69]. Another mechanism for the dispersal of charge from cations of high charge density is the ionization of a bound water molecule to produce bound HO^- and

free H^+; the lowest pK_a for water attached to Cr^{3+} is 4.29 [23]. Estimated pK_a values for most aqua metal ions are available [10,23]. Circumstantial evidence for charge transfer to solvent from F^- by $^{19}F^-$ nuclear magnetic resonance and from phosphate by ^{31}P nuclear magnetic resonance and other techniques has been reviewed [70]. The phenomenon of charge transfer to solvent [70,71] is also the most likely basis for the polyelectrolyte behavior of nucleic acids [72].

iii. Ion–solvent interactions can be accurately represented by a point charge–water dipole interaction. However, the neutron diffraction studies of Powell et al. [73] establish that the H_2O interacts with Cl^- via a nearly linear hydrogen bond and not a dipolar interaction. In addition, large monovalent cations of low charge density the size of K^+ and larger do not orient the adjacent water molecules [13], while small cations of high charge density the size of Na^+ and smaller transfer substantial charge to the tightly bound water molecules—see above [50]. Ab initio molecular orbital calculations of metal ion monohydrates indicate that ''The bonding of the water molecule, although electrostatic in origin, is…more complex than a simple interaction between a point charge on the metal ion, and the water dipole'' [74]. We thus conclude that a point charge–water dipole interaction is not an accurate description of ion–water interactions under any circumstances.

iv. Ion–water interactions are strong relative to water–water interactions. Consider each of the IA cations (H^+, Li^+, Na^+, K^+, Rb^+, Cs^+, Fr^+) and VIIA halides (F^-, Cl^-, Br^-, I^-, At^-) to be a point charge at the center of a sphere of the appropriate size. As the sphere becomes larger, the point charge eventually becomes distant enough from the water molecules at the surface of the sphere that the ion–water interactions are weaker than the water–water interactions in bulk solution. This is the simplest description of a chaotrope. Chaotropes are large monovalent ions of low charge density the size of K^+ or larger for cations [13,31], and the size of Cl^- or larger for anions [14,29]. To assume that ion–water interactions are strong relative to water–water interactions is to assume that chaotropes do not exist. However, since all the positive charges of proteins reside on amino groups, which are derivatives of the chaotrope NH_4^+ [14,18,30], since the major intracellular monovalent cation is the chaotrope K^+, and since the major extracellular monovalent anion is the chaotrope Cl^-, this is a serious distortion [14]. Continuum electrostatics predicts that all ions in water will be *repelled* from a non-polar surface via image forces, but experimentally chaotropes are found to *adsorb* to non-polar surfaces, the driving force for adsorption being the release of weakly bound water adjacent to the ion to become strongly interacting water in bulk solution [15,18].

v. Positive and negative ions of the same total charge have equivalent interactions with the solvent. However, anions are experimentally found to be more strongly hydrated than cations of the same charge density [18].

vi. The effects of ions in solution are due to long-range electric field effects. In contrast, neutron and X-ray diffraction experiments find no large effects on the density of water outside of the first hydration layer for ions of charge density equal to or less than that of Mg^{2+}, and they find large effects on the second hydration layer only for trivalent cations, such as Cr^{3+} [13,38,39]. Neutron diffraction of ions in D_2O generates radial distribution functions containing separate peaks for solvent oxygen and deuterium in the vicinity of the ion, yielding information on the orientation of the solvent [13]. Li^+, which causes a large solvent density perturbation, generates separate peaks for solvent oxygen (near the ion) and deuterium (further away from the ion), showing strong orientation of the bound D_2O. Ag^+ (an analog of Na^+), which causes moderate solvent-density perturbation, generates partially resolved peaks for oxygen and deuterium, indicating partial orientation of the adjacent D_2O. In contrast, K^+ (which is weakly hydrated [14]) causes only a small solvent-density perturbation with no separation of the peaks for oxygen and deuterium, indicating no orientation of the adja-

cent solvent. Thus, preferential orientation of solvent near cations disappears when the solvent density perturbation disappears, and solvent density perturbation is probably a meaningful measure of the distance over which the electric field of the ion has a substantial effect on water behavior. In fact, the weakly hydrated Cl^- anion [14] causes significant solvent density perturbation and surprisingly orients the adjacent water molecules [13], even though this oriented water is not tightly held [29]; therefore, solvent density perturbation detects electric field effects on water, even when they are weaker than water–water interactions. Since solvent density perturbations correlate well with strongly bound water as measured by Sephadex G-10 chromatography, we conclude that substantial electric field effects do not extend beyond the hydration effects.

It should also be pointed out that, although the concept of 'ionic strength' was not formulated in terms of the model of continuum electrostatics, it also ignored the issue of charge density, treating all ions of the same total charge and sign equivalently. Furthermore, while it did not distinguish between *direct* interactions between the ions of the supporting electrolyte and the test solute (inner sphere coordination) and *indirect* interactions (mediated via intervening water molecules), it implicitly refers to indirect interactions. Inner-sphere ion pair formation (direct interaction) is now known to occur when oppositely charged ions have matching absolute free energies of hydration, because inner-sphere ion pair formation is a dehydration, and the energetic cost of the dehydration cannot exceed the energetic gain of ion pair formation [14]; salt effects on biological macromolecules are typically a mixture of direct and indirect effects [75,76].

3.7. Ionic strength arises from hydration forces

NaCl is typically used to establish a given 'ionic strength' for some measurement in solution, and then salts containing more highly charged species, such as Na_2HPO_4, Na_2SO_4 and $CaCl_2$, are substituted for all or part of the NaCl to produce the same ionic strength, sometimes at a different pH. Table 3 shows that the ratio of the hydrated volume of di-anionic HPO_4^{2-} and di-anionic SO_4^{2-} to the hydrated volume of mono-anionic Cl^- is approximately 4, the ratio of their charges squared as specified in the equation for ionic strength. Similarly, the ratio of the hydrated volumes of Ba^{2+}, Ca^{2+} and Cr^{3+} to that of Na^+ also approximates the ratio of their charges squared. This suggests that the phenomena described by the empirical formula for ionic strength largely arise from local effects related to the size of the hydrated ion, such as space filling, osmotic, water activity, surface tension and hydration shell overlap effects rather than from long-range electric field effects. The water molecule has been modeled as a zwitterionic tetrahedron with two -0.17 charges and two $+0.17$ charges [77], and as a zwitterion with a full negative and full positive charge [14]. These models emphasize the direct electrostatic interactions between the local charge on zwitterionic water and other water molecules and ions rather than treating water as a dielectric continuum, and they suggest that the strongest electrostatic interactions of an ion in water will always be with its nearest neighbors. The almost complete dissociation of soluble neutral salts in water implies that the strength of ion–water interactions is comparable to the strength of hydrated ion–hydrated ion interactions. Aqueous solutions of ions differ from aqueous solutions of neutral solutes in having a requirement for overall net neutrality, showing

Table 3
The ratio of the square of the charge (z^2) on two ions is approximately equal to the ratio of their hydrated volumes (V_h)

Ion	$\frac{V_h^{ion}}{V_c^{Cl}}$	$\frac{V_h^{ion}}{V_c^{Na}}$	$\frac{(z_{ion})^2}{(z_{Na\ or\ Cl})^2}$
Cl^-	1.00		1
HPO_4^{2-}	4.72		4
SO_4^{2-}	3.64		4
Na^+		1.00	1
Ba^{2+}		5.17	4
Ca^{2+}		3.03	4
Cr^{3+}		8.10	9

$V_h^{ion} = 4/3\pi r_h^3$; $V_h^{Cl} = 4/3\pi r_{h\text{-}Cl}^3$; $V_h^{Na} = 4/3\pi r_{h\text{-}Na}^3$.

local preferential interactions with other charge centers, and producing substantial charge transfer to solvent from ions of high charge density [70]; there is no evidence for substantial long-range electric field effects. This perspective naturally follows from realizing that ions are not point charges—the electric charge of ions in water is always delocalized over a significant volume—and that water behaves more as a zwitterion participating in local electrostatic and partially covalent bonds than as a dielectric continuum participating in dipolar interactions.

3.8. The importance of second shell water (the 'transition layer') in aqueous solution

Space filling effects (also known as excluded volume effects) [78,79] appear to be a major component of the thermodynamic non-ideality associated with neutral solutes [80], with osmotic effects playing a smaller role. However, the gas-phase experiments of Kebarle and co-workers [81,82] demonstrate that the second-shell water (each shell being one water molecule thick) makes a far greater contribution to the total absolute free energy of solvation for K^+ and for Cl^- than is the case with other solvents because of the small size of water (bringing the second shell closer to the ion), the capacity of water to both accept and donate strong hydrogen bonds, and the ability of water to make effective hydrogen bonds in geometrically restricted regions. Markham et al. [83] used ab initio molecular orbital calculations to show that the first hydration shell of Mg^{2+} contributes approximately 60% of the free energy of hydration, with the second layer contributing most of the rest, even though the second layer is not tightly held (Table 1 and [38]). For simplicity, we present in Fig. 2 a picture that is similar to our earlier model of solute hydration [70]. Adjacent to the test solute is a solvation layer, usually one water molecule thick. The behavior of the water in the solvation layer is controlled by the test solute (this does not require that any or all of the solvation layer be tightly bound). Adjacent to the solvation layer is the transition layer, one water molecule thick, which competes for hydrogen bonding interactions with both the solvation layer and the bulk surface; it makes a large contribution to the absolute free energy of hydration of the solute, even though it is not strongly bound to the solute. Adjacent to the transition layer is the bulk surface, the behavior of which is largely controlled by the bulk solution. The transition layer, which has been detected by X-ray diffraction of $Zn(NO_3)_2$ in water [40], appears to arise from strongly coupled local interactions as opposed to long-range effects, since Table 1 indicates that only two of the six solvation-layer water molecules of Zn^{2+} are tightly held. Other evidence suggesting the presence of a transition layer in aqueous solutions includes high-resolution neutron quasi-elastic scattering of Mg^{2+} and Ni^{2+} solutions [84] and the temperature dependence of Hofmeister effects [70]. In concentrated solutions, when the water strongly bound to ions (as measured by the apparent dynamic hydration number in Table 1) displaces the transition layer of a test solute (Fig. 2), the solubility of the test solute is decreased because the water strongly bound to ions is 'not available' to help stabilize the solvation layer of the test solute [70]. These hydration-shell overlap effects appear to be a principal mechanism for the indirect interactions that underlie stabilization of protein structure and decrease of protein solubility by strongly hydrated salts and neutral solutes [70],

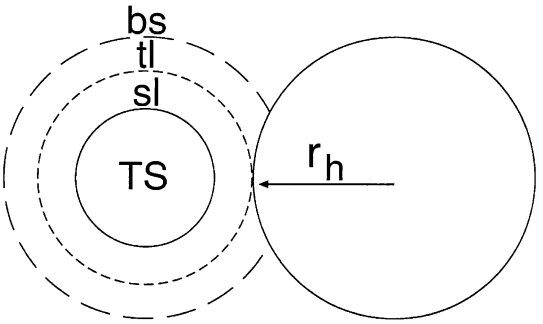

Fig. 2. Hydration shell overlap effects: strongly hydrated ions decrease the solubility of test solutes by displacement of the transition layer. TS, test solute; sl, solvation layer (which may be strongly or weakly held); tl, transition layer (which is weakly held); bs, bulk surface; r_h, radius of equivalent hydrated sphere (determined for strongly hydrated ions using the apparent molecular weight of the ion on a Sephadex G-10 size-exclusion column at 30 °C and atmospheric pressure).

and provide an alternative explanation for ionic strength effects that is consistent with a large body of physical data on aqueous solutions.

Acknowledgments

We thank the National Aeronautics and Space Administration (NASA) for supporting this work through grant NAG 8 1573 for fundamental research on the basis of protein stability and solubility. We also thank several colleagues who read several drafts of this paper.

References

[1] A. McPherson, A comparison of salts for the crystallization of macromolecules, Protein Sci. 10 (2001) 418–422.
[2] M. Ries-Kautt, A. Ducruix, Inferences drawn from physicochemical studies of crystallogenesis and precrystalline state, Methods Enzymol. 276 (1997) 23–59.
[3] E. Karlsson, L. Ryden, J. Brewer, Ion-exchange chromatography, in: J.-C. Janson, L. Ryden (Eds.), Protein Purification. Principles, High-Resolution Methods and Applications, Wiley-VCH, New York, 1998, pp. 145–205.
[4] W.R. Melander, D. Corradini, C. Horvath, Salt-mediated retention of proteins in hydrophobic-interaction chromatography. Application of solvophobic theory, J. Chromatogr. 317 (1984) 67–85.
[5] A.A. Zavitsas, Properties of water solutions of electrolytes and non-electrolytes, J. Phys. Chem. B 105 (2001) 7805–7817.
[6] T. Osakai, A. Ogata, K. Ebina, Hydration of ions in organic solvent and its significance in the Gibbs energy of ion transfer between two immiscible liquids, J. Phys. Chem. B 101 (1997) 8341–8348.
[7] E.S. Amis, Solvation of ions, in: M.R.J. Dack (Ed.), Solutions and Solubilities, Part 1, Wiley Interscience, 1975.
[8] P.P.S. Saluja, Environment of ions in aqueous solutions, International Review of Science: Physical Chemistry, 1976, pp. 1–51.
[9] J. Celeda, On theory of ionic volumes in dilute aqueous solutions of electrolytes, Collect. Czech. Chem. Commun. 53 (1988) 433–445.
[10] J. Burgess, Ions in Solution: Basic Principles of Chemical Interactions, Horwood Publishing Limited, 1999.
[11] Y. Marcus, A simple empirical model describing the thermodynamics of hydration of ions of widely varying charges, sizes and shapes, Biophys. Chem. 51 (1994) 111–127.
[12] J. Kielland, Individual activity coefficients of ions aqueous solutions, J. Am. Chem. Soc. 59 (1937) 1675–1678.
[13] J.E. Enderby, Ion solvation via neutron scattering, Chem. Soc. Rev. 24 (1995) 159–168.
[14] K.D. Collins, Charge density-dependent strength of hydration and biological structure, Biophys. J. 72 (1997) 65–76.
[15] M.W. Washabaugh, K.D. Collins, The systematic characterization by aqueous column chromatography of solutes which affect protein stability, J. Biol. Chem. 261 (1986) 12477–12485.
[16] N.V.B. Marsden, Tritium exchanges in Sephadex G-10, J. Chromatogr. 58 (1971) 304–306.
[17] Z. Marczenko, Separation and Spectrophotometric Determination of Elements, Wiley, New York, 1986.
[18] K.D. Collins, Sticky ions in biological systems, Proc. Natl. Acad. Sci. USA 92 (1995) 5553–5557.
[19] H.G. Hertz, Nuclear magnetic relaxation spectroscopy, in: F. Franks (Ed.), Aqueous Solutions of Simple Electrolytes, Plenum Press, New York, 1973.
[20] R.W. Impey, P.A. Madden, I.R. McDonald, Hydration and mobility of ions in solution, J. Phys. Chem. 87 (1983) 5071–5083.
[21] G.W. Neilson, J.E. Enderby, The coordination of metal aquaions, Adv. Inorg. Chem. 34 (1989) 195–218.
[22] L. Helm, A.E. Merbach, Water exchange on metal ions: experiments and simulations, Coord. Chem. Rev. 187 (1999) 151–181.
[23] D.T. Richens, The Chemistry of Aqua Ions. Synthesis, Structure and Reactivity: A Tour through the Periodic Table of the Elements, Wiley, New York, 1997.
[24] F.A. Cotton, G. Wilkinson, C.A. Murillo, M. Bochmann, Advanced Inorganic Chemistry, Wiley Interscience, 1999.
[25] G.K. Ackers, Molecular sieve methods of analysis, in: H. Neurath, R.L. Hill (Eds.), The Proteins, Academic Press, New York, 1975, pp. 1–94.
[26] F. Avbelj, P. Luo, R.L. Baldwin, Energetics of the interaction between water and the helical peptide group and its role in determining helix propensities, Proc. Natl. Acad. Sci. USA 97 (2000) 10786–10791.
[27] W.A.P. Luck, How to understand liquids, in: P.L. Huyskens, W.A.P. Luck, T. Zeegers-Huyskens (Eds.), Intermolecular Forces. An Introduction to Modern Methods and Results, Springer-Verlag, New York, 1991, pp. 55–78.
[28] L. Pauling, The Nature of the Chemical Bond, Cornell University Press. 3rd edition (1960).
[29] G.W. Neilson, J.E. Enderby, The structure of an aqueous solution of nickel chloride, Proc. R. Soc. Lond. A 390 (1983) 353–371.
[30] P.A.M. Walker, D.G. Lawrence, G.W. Neilson, J. Cooper, The structure of concentrated aqueous ammonium nitrate solutions, J. Chem. Soc. Faraday Trans. 185 (1989) 1365–1372.
[31] N.T. Skipper, G.W. Neilson, X-Ray and neutron diffraction studies on concentrated aqueous solutions of sodium nitrate and silver nitrate, J. Phys. Condens. Matter 1 (1989) 4141–4154.

[32] R.C. Weast (Ed.), CRC Handbook of Chemistry and Physics, 56th ed., CRC Press, Cleveland, 1975, p. F-11.
[33] K. Lonsdale, The structure of ice, Proc. R. Soc. Lond. A 247 (1958) 424–434.
[34] M. Gerstein, J. Tsai, M. Levitt, The volume of atoms on the protein surface: calculated from simulation, using Voronoi polyhedra, J. Mol. Biol. 249 (1995) 955–966.
[35] G. Hefter, Y. Marcus, A critical review of methods for obtaining ionic volumes in solution, J. Solut. Chem. 26 (1997) 249–266.
[36] C.S. Babu, C. Lim, Theory of ionic hydration: insight from molecular dynamics simulations and experiments, J. Phys. Chem. B 103 (1999) 7958–7968.
[37] K. Heremans, The behaviour of proteins under pressure, in: R. Winter, J. Jonas (Eds.), High Pressure Chemistry, Biochemistry and Material Science, Kluwer Academic Publishers, Dordrecht, 1993, pp. 443–469.
[38] N.T. Skipper, G.W. Neilson, S.C. Cummings, An X-ray diffraction study of $Ni^{2+}_{[aq]}$ and $Mg^{2+}_{[aq]}$ by difference methods, J. Phys. Condens. Matter 1 (1989) 3489–3506.
[39] R.D. Broadbent, G.W. Neilson, M. Sandstrom, The hydration structure of Cr^{3+} in a concentrated aqueous solution, J. Phys. Condens. Matter 4 (1992) 639–648.
[40] A. Munoz-Paez, R.R. Pappalardo, E.S. Marcos, Determination of the second hydration shell of Cr^{3+} and Zn^{2+} in aqueous solutions by extended X-ray absorption fine structure, J. Am. Chem. Soc. 117 (1995) 11710–11720.
[41] C.W. Bock, J.P. Glusker, Organization of water around a beryllium cation, Inorg. Chem. 32 (1993) 1242–1250.
[42] B. Schneider, K. Patel, H.M. Berman, Hydration of the phosphate group in double-helical DNA, Biophys. J. 75 (1998) 2422–2434.
[43] G.A. Jeffrey, H. Maluszynska, A survey of hydrogen bond geometries in the crystal structures of amino acids, Int. J. Biol. Macromol. 4 (1982) 173–185.
[44] C.H. Gorbitz, M.C. Etter, Hydrogen bonds to carboxylate groups. The questions of three-centre interactions, J. Chem. Soc. Perkin Trans. 2 (1992) 2131–2135.
[45] G.D. Markham, C.L. Bock, C.W. Bock, Hydration of the carboxylate group: an ab initio molecular orbital study of acetate–water complexes, Struct. Chem. 8 (1997) 293–307.
[46] A. Kamitakahara, J. Pranata, A computational model for the stereoelectronic effects of carboxylate lone pairs, Bioorg. Chem. 23 (1995) 256–262.
[47] R.S. Alexander, Z.F. Kanyo, L.E. Chirlian, D.W. Christianson, Stereochemistry of phosphate–Lewis acid interactions: implications for nucleic acid structure and recognition, J. Am. Chem. Soc. 112 (1990) 933–937.
[48] L. Chertanova, C. Pascard, Statistical analysis of noncovalent interactions of anion groups in crystal structures. I. Hydrogen bonding of sulfate anions, Acta Crystallogr. B 52 (1996) 677–684.
[49] N.A. Hewish, G.W. Neilson, J.E. Enderby, Environment of Ca^{2+} ions in aqueous solvent, Nature 297 (1982) 138–139.
[50] C.W. Bock, A. Kaufman, J.P. Glusker, Coordination of water to magnesium cations, Inorg. Chem. 33 (1994) 419–427.
[51] M.C. Read, M. Sandstrom, Second-sphere hydration of rhodium (III) and chromium (III) in aqueous solution. A large-angle X-ray scattering and EXAFS study, Acta Chem. Scand. 46 (1992) 1177–1182.
[52] A. Bleuzen, F. Foglia, E. Furet, L. Helm, A.E. Merbach, J. Weber, Second coordination shell water exchange rate and mechanism: experiments and modeling on hexaaquachromium, J. Am. Chem. Soc. 118 (1996) 12777–12787.
[53] J.M. Martinez, R.R. Pappalardo, E.S. Marcos, K. Refson, S. Diaz-Moreno, A. Munoz-Paez, Dynamics of a highly charged ion in aqueous solutions: MD simulations of dilute $CrCl_3$ aqueous solutions using interaction potentials based on the hydrated ion concept, J. Phys. Chem. B 102 (1998) 3272–3282.
[54] D. Jamroz, M. Wojcik, J. Lindgren, Solvation of Cr^{3+} cation in water–acetonitrile mixture studied by IR spectroscopy: molecular penetration into the solvation shells, Spectrochim. Acta A: Mol. Biomol. Spectrosc. 56A (2000) 1939–1948.
[55] P.A. Bergstrom, J. Lindgren, M.C. Read, M. Sandstrom, Infrared spectroscopic evidence for second-sphere hydration in aqueous solutions of Al^{3+}, Cr^{3+}, and Rh^{3+}, J. Phys. Chem. 95 (1991) 7650–7655.
[56] G. Zundel, Easily polarizable hydrogen bonds—their interactions with the environment—IR continuum and anomalous large proton conductivity, in: P. Schuster, G. Zundel, C. Sandorfy (Eds.), The Hydrogen Bond—Recent Developments in Theory and Experiments. II. Structure and Spectroscopy, North-Holland, Amsterdam, 1976, pp. 683–766.
[57] M. Eigen, Proton transfer, acid–base catalysis and enzymatic hydrolysis, Angew. Chem. Int. Ed. 3 (1964) 1–19.
[58] R. Vuilleumier, D. Borgis, Quantum dynamics of an excess proton in water using an extended empirical valence-bond Hamiltonian, J. Phys. Chem. B 102 (1998) 4261–4264.
[59] R. Vuilleumier, D. Borgis, An extended empirical valence bond model for describing proton mobility in water, Isr. J. Chem. 39 (1999) 457–467.
[60] U.W. Schmitt, G.A. Voth, Quantum properties of the excess proton in liquid water, Isr. J. Chem. 39 (1999) 483–492.
[61] M. Tuckerman, K. Laasonen, M. Sprik, M. Parrinello, Ab initio molecular dynamics simulation of the solvation and transport of H_3O^+ and OH^- ions in water, J. Phys. Chem. 99 (1995) 5749–5752.
[62] J.J. Novoa, F. Mota, C. Perez del Valle, M. Planas, Structure of the first solvation shell of the hydroxide anion. A model study using $OH^-(H_2O)_n$ ($n=4$, 5, 6,

7, 11, 17) clusters, J. Phys. Chem. A 101 (1997) 7842–7853.
[63] J.R. Pliego, J.M. Riveros, On the calculation of the absolute solvation free energy of ionic species: application of the extrapolation method to the hydroxide ion in aqueous solution, J. Phys. Chem. B 104 (2000) 5155–5160.
[64] J. Choi, N. Hirota, M. Terazima, A pH-jump reaction studied by the transient grating method: photodissociation of *o*-nitrobenzaldehyde, J. Phys. Chem. A 105 (2001) 12–18.
[65] C. Klofutar, D. Rudan-Tasic, V. Mancic-Klofutar, Partial molar volumes of tetraalkylammonium hydroxides in aqueous solutions at 25 °C, J. Solut. Chem. 26 (1997) 1037–1047.
[66] G.N. Lewis, M. Randall, The activity coefficient of strong electrolytes, J. Am. Chem. Soc. 43 (1921) 1112–1154.
[67] P. Debye, E. Hückel, On the theory of electrolytes. I. Freezing point depression and related phenomena, Phys. Z. 24 (1923) 185–206.
[68] P. Debye, E. Hückel, On the theory of electrolytes. II. Limiting law for electric conductivity, Phys. Z. 24 (1923) 305–325.
[69] H. Suga, J.A. Cowan, J.W. Szostak, Unusual metal ion catalysis in an acyl-transferase ribozyme, Biochemistry 37 (1998) 10118–10125.
[70] K.D. Collins, M.W. Washabaugh, The Hofmeister effect and the behaviour of water at interfaces, Q. Rev. Biophys. 18 (1985) 323–422.
[71] V. Gutmann, The Donor–Acceptor Approach to Molecular Interactions, Plenum Press, New York, 1978.
[72] M.T. Record, W. Zhang, C.F. Anderson, Analysis of effects of salts and uncharged solutes on protein and nucleic acid equilibria and processes: a practical guide to recognizing and interpreting polyelectrolyte effects, Hofmeister effects, and osmotic effects of salts, Adv. Protein Chem. 51 (1998) 281–353.
[73] D.H. Powell, G.W. Neilson, J.E. Enderby, The structure of Cl^- in aqueous solution: an experimental determination of $g_{ClH}(r)$ and $g_{ClO}(r)$, J. Phys. Condens. Matter 5 (1993) 5723–5730.
[74] M. Trachtman, G.D. Markham, J.P. Glusker, P. George, C.W. Bock, Interactions of metal ions with water: ab initio molecular orbital studies of structure, bonding enthalpies, vibrational frequencies and charge distributions. 1. Monohydrates, Inorg. Chem. 37 (1998) 4421–4431.
[75] J.G. Norby, M. Esmann, The effect of ionic strength and specific anions on substrate binding and hydrolytic activities of Na,K-ATPase, J. Gen. Physiol. 109 (1997) 555–570.
[76] B.A. Pederson, M.A. Nordlie, J.D. Foster, R.C. Nordlie, Effects of ionic strength and chloride ion on activities of the glucose-6-phosphatase system: regulation of the biosynthetic activity of glucose-6-phosphatase by chloride ion inhibition/deinhibition, Arch. Biochem. Biophys. 353 (1998) 141–151.
[77] A. Ben-Naim, F.H. Stillinger, Aspects of the statistical–mechanical theory of water, in: R.A. Horne (Ed.), Water and Aqueous Solutions. Structure, Thermodynamics, and Transport Processes, Wiley Interscience, 1972.
[78] A.P. Minton, The influence of macromolecular crowding and macromolecular confinement on biochemical reactions in physiological media, J. Biol. Chem. 276 (2001) 10577–10580.
[79] R.J. Ellis, Macromolecular crowding: obvious but underappreciated, Trends Biochem. Sci. 26 (2001) 597–604.
[80] P.R. Davis-Searles, A.J. Saunders, D.A. Erie, D.J. Winzor, G.J. Pielak, Interpreting the effects of small uncharged solutes on protein-folding equilibria, Annu. Rev. Biophys. Biomol. Struct. 30 (2001) 271–306.
[81] J. Sunner, P. Kebarle, Ion–solvent molecule interactions in the gas phase. The potassium ion and Me2SO, DMA, DMF, and acetone, J. Am. Chem. Soc. 106 (1984) 6135–6139.
[82] T.F. Magnera, G. Caldwell, J. Sunner, S. Ikuta, P. Kebarle, Solvation of the halide anions in dimethyl sulfoxide. Factors involved in enhanced reactivity of negative ions in dipolar aprotic solvents, J. Am. Chem. Soc. 106 (1984) 6140–6146.
[83] G.D. Markham, J.P. Glusker, C.L. Bock, M. Trachtman, C.W. Bock, Hydration energies of divalent beryllium and magnesium ions: an ab initio molecular orbital study, J. Phys. Chem. A 100 (1996) 3488–3497.
[84] N.A. Hewish, J.E. Enderby, W.S. Howells, The dynamics of water molecules in ionic solution, J. Phys. C: Solid-State Phys. 16 (1983) 1777–1791.
[85] J.E. Enderby, Electrolyte Monograph, University of Bristol Department of Physics, H.H. Wills Physics Laboratory, Bristol, UK, (1993).